

Multiplicity per rapidity in Carruthers and hadron resonance gas approaches

Abdel Nasser Tawfik*

*Nile University - Egyptian Center for Theoretical Physics (ECTP),
Juhayna Square off 26th-July-Corridor, 12588 Giza, Egypt*

Mahmoud Hanafy

*Physics Department, Faculty of Science, Benha University, 13518, Benha, Egypt and
World Laboratory for Cosmology And Particle Physics (WLCAPP), 11571 Cairo, Egypt*

Werner Scheinast

*Joint Institute for Nuclear Research - Veksler and Baldin Laboratory
of High Energy Physics, Moscow Region, 141980 Dubna, Russia*

(Dated: November 6, 2019)

The multiplicity per rapidity of the well-identified particles π^- , π^+ , k^- , k^+ , \bar{p} , p , and $p-\bar{p}$ measured in different high-energy experiments, at energies ranging from 6.3 to 5500 GeV, are successfully compared with the Cosmic Ray Monte Carlo (CRMC) event generator. For these rapidity distributions, we introduce a theoretical approach based on fluctuations and correlations (Carruthers) and another one based on statistical thermal assumptions (hadron resonance gas model). Both approaches are fitted to the two sets of results deduced from experiments and simulations. We found that the Carruthers approach reproduces well the full range of multiplicity per rapidity for all produced particles, at the various energies, while the HRG approach fairly describes the results within a narrower rapidity-range. While the Carruthers approach seems to match well with the Gaussian normal distribution, ingredients such as flow and interactions should be first incorporated in the HRG approach.

PACS numbers:

Keywords: Carruthers and thermal rapidity distributions, Multiplicity per rapidity, CRMC/EPOS1hc event generator

*Electronic address: atawfik@nu.edu.eg

I. INTRODUCTION

Characterizing the particle production is seen as one of the main goals of the relativistic heavy-ion experiments [1]. By investigating the properties of the different produced particles throughout the various stages of the nuclear collision, essential information on partonic such as quark gluon-plasma (QGP) and on hadronic phases can be obtained [2–7]. The sophisticated nuclear process starting from deconfined QGP and going through phase transition into confined hadrons, or vice versa is - among others - characterized by a final stage, at which the number of the produced particles is conjectured to be fixed (chemically frozen) [8]. The information, which can be deduced from the different experiments such as the ones at the Super Proton-synchrotron (SPS) at CERN, the Relativistic Heavy Ion Collider (RHIC) at BNL, and the Large Hadron Collider (LHC) at CERN, on the characterization of the particle distributions and the dynamical evolution of such strongly interacting systems, for instance, elliptic and radial flow, manifests an essential property of the particle spectra [9]. Various quantities such as particle ratios, transverse mass spectra, and multiplicity per rapidity are also crucial in studying dynamics and different general properties, especially at the freezeout stage [10].

The rapidity distribution, for example, was studied in different approaches [11–28]. Assuming superposition of two fireballs along the rapidity axes, the Tsallis-type distribution was assumed to give a successful description for the rapidity distribution [12]. A thermodynamically consistent excluded volume model, in which flow is included, was proposed to well reproduce the rapidity distribution [9, 13]. A relative better description was obtained when longitudinal collective flow and excluded volume corrections have been taken into consideration [15, 16]. Impacts of the hydrodynamic flow have been introduced in refs. [17, 18]. In [19, 20]. In a single statistical thermal freezeout model based on a single set of parameters, the rapidity distribution was fairly analyzed [21]. Also, in a hydrodynamical model with single particle spectra, the rapidity distribution was studied [22, 25]. The rapidity distribution was estimated in hydrodynamic models [23]. Extended statistical hadronization models have been utilized in describing the rapidity distribution [24]. In [26, 27], an extended thermal model is used to calculate particle spectra, at RHIC energies. In ref. [28], the rapidity distribution was calculated assuming longitudinal hydrodynamic expansion of fluid created in the heavy-ion collisions.

In statistical models [26–31], the chemical potential μ was successfully related to the rapidity y . Accordingly, the rapidity distribution could be calculated over a wide large range of rapidity [31]. An extended longitudinal scaling was also introduced to the thermal model [30].

It is well known that the distributions of the various particles are not isotropic. Thus, it is obvious

to conclude that the multiplicity per rapidity calculated within the hadron resonance gas (HRG) model should not convincingly reproduce the experimental results, especially at a wide range of rapidity [13]. The inclusion of heavy resonances with their decay channels likely improves the HRG reproduction of the measured rapidity multiplicities. The best HRG results are the ones within small-rapidity region. The present script presents other alternatives aiming at improving HRG [32–43]. We also confront our results to the predictions from the Cosmic Ray Monte Carlo (CRMC) event generator [44–53], at energies ranging from 6.3 up to 5500 GeV. The CRMC event generator includes various hadronic interaction models such as EPOS1.99 and EPOS1hc models. In this context, We use EPOS1hc hadronic interaction model from high down to low energies.

For rapidity distributions measured in high-energy collisions and/or simulated in CRMC, we propose the utilization of Carruthers approach, which is based on hierarchy of cumulant correlation functions and their linked-pair approximation. This approach assumes an approximate translation invariance and utilizes a linking of averaged factorial moments to the second-order experimental moment in the final state of the particle production. For rapidity histograms, the various bins are assumed being irregular, i.e. they are influenced by fractal attractor or have an intermittent nature. The full range of rapidity $(\Delta y)^p$ can be then divided into smaller hypercubes of size $(\delta y)^p$ and thus the ordinary bin-averaged factorial moments can be determined, which - in turn - can be expressed in a linked-pair approximation. Relating this to the negative binomial distribution makes it possible to propose a specific functional form such as Gaussian or a general exponential for the cumulants.

The present paper is organized as follows. We briefly introduce Carruthers and HRG approaches in section II. The results are discussed in section IV. The conclusions are outlined in section V.

II. MODELS

In this section, we give a brief description for the particle multiplicity as deduced from the HRG approach which is based on statistical thermal assumptions and the Carruthers approach which is based on correlations and fluctuations.

A. HRG approach for rapidity multiplicity

It is widely known that the formation of resonances could be understood as bootstrap, i.e. the fireballs or resonances are demonstrated to be consisting of more smaller fireballs or lighter resonances, which - in turn - are composed of smaller fireballs and lighter resonances etc. For such a system, the

thermodynamics quantities can be derived directly from the partition function $Z(T, \mu, V)$. In a Grand canonical ensemble, the partion function reads [1]

$$Z(T, V, \mu) = \text{Tr} \left[\exp \left(\frac{\mu N - H}{T} \right) \right], \quad (1)$$

where H is Hamiltonian of the system, N is the total number of constituents. In the HRG model, Eq. (1) can be expressed as a sum over all hadron resonances¹

$$\ln Z(T, V, \mu) = \sum_i \ln Z_i(T, V, \mu) = \frac{V g_i}{(2\pi)^3} \int_0^\infty \pm d^3 p \ln \left[1 \pm \exp \left(\frac{\varepsilon_i(p) - \mu_i}{T} \right) \right], \quad (2)$$

where \pm stands for bosons and fermions, respectively and $\varepsilon_i = (p^2 + m_i^2)^{1/2}$ is the dispersion relation of the i -th particle, for which the total number of particles can be obtained as

$$N_i = T \frac{\partial Z_i(T, V)}{\partial \mu_i} = \frac{V g_i}{(2\pi)^3} \int_0^\infty d^3 p \left[\exp \left(\frac{\varepsilon_i(p) - \mu_i}{T} \right) \pm 1 \right]^{-1}. \quad (3)$$

From Eq. (3), the invariant momentum spectrum of particles emitted from a thermal source can be derived [56, 57]

$$\varepsilon_i \frac{d^3 N_i}{dy m_T dm_T d\phi} = \varepsilon_i \frac{V g_i}{(2\pi)^3} \left[\exp \left(\frac{\varepsilon_i(p) - \mu_i}{T} \right) \pm 1 \right]^{-1}, \quad (4)$$

where m_T is the transverse mass and is given by $m_T = \sqrt{m^2 + p_T^2}$, where p_T is the transverse momentum. The energy of the i -th particle, ε_i , can be then expressed in terms of the rapidity (y) and m_T as $\varepsilon = m_T \cosh(y)$. Through integration over the full transverse mass m_T , the multiplicity N per rapidity y can be derived,

$$\frac{dN}{dy} = \sum_i \frac{V g_i}{(2\pi)^2} \int_0^\infty \cosh(y) m_T^2 \left[\exp \left(\frac{m_T \cosh(y) - \mu_i}{T} \right) \pm 1 \right]^{-1}. \quad (5)$$

Eq. (5) can be rewritten as

$$\frac{dN}{dy} = \sum_i \frac{V g_i}{(2\pi)^2} T [m_T + 2T \operatorname{sech}(y) (m_T + T \operatorname{sech}(y))] \exp \left[-\frac{m_T \cosh(y) - (\mu_i \pm 1)}{T} \right], \quad (6)$$

where T is the freezeout temperature, μ_i is the chemical potential which can be related to the beam energy [1, 58], g_i is the degeneracy, and V is the volume of the fireball. Eq. (6) gives the multiplicity per rapidity for hadron states, whereas combination of the trigonometric functions sech and \cosh are conjectured to assure Gaussian-like distribution function. In classical statistics, Eq. (6) can be reexpressed as

$$\frac{dN}{dy} = \sum_i \frac{TV g_i}{(4\pi)^2} (2T^2 + m_T \cosh(y) (2T + m_T \cosh(y))) \operatorname{sech}(y^2) \exp \left(\frac{\mu_i - m_T \cosh(y)}{T} \right). \quad (7)$$

¹ either compiled by the particle data group [54] or still theoretical predictions [55].

B. Carruthers approach for rapidity multiplicity

Suppose we have a histogram for rapidity, y , describing an event, l , in the rapidity interval Δy , which is divided into X bins of length δy . Consequently, the rapidity interval reads $\Delta y = X\delta y$. In the thermal models, the rapidity density of i -th particle is given as two-particle correlation integral [59]

$$\frac{dN^l(y)}{dy} = \int_{\delta y} \rho^l(y) dy, \quad (8)$$

where $\rho^l(y)$ is the probability density corresponding to the considered regions (*fireballs*) of the latest (final) hadron yields. This probability density $\rho^l(y)$ can be expressed as [59]

$$\rho^l(y) = \sum_{\mathbf{i}} \delta(y - y_{\mathbf{i}}^l), \quad (9)$$

in which $\delta(y - y_{\mathbf{i}}^l)$ counts the available number of points $y_{\mathbf{i}}^l$ in the known interval δy for l -th event, i.e. δ -function defines the rapidity bin width. For many events, the single particle density dN/dy related to the differential cross-section $d\sigma/dy$ reads [59]

$$\frac{1}{\sigma_{\mathbf{i}}} \frac{d\sigma}{dy} = \frac{1}{N^l} \sum_{\mathbf{1}} \frac{dN^l}{dy} \quad (10)$$

where N^l is the total number of particles and $\sigma_{\mathbf{i}}$ is the corresponding cross-section. This can be converted into a statistical ensemble having a probability density $\rho(y_1, y_2, \dots, y_N)$ for the distributed points $y_{\mathbf{i}}$, where $i = 1, 2, \dots, N$ stand for particles within the interval Δy . Thus, Eq. (10) can be rewritten as [59]

$$\begin{aligned} \frac{1}{\sigma_{\mathbf{i}}} \frac{d\sigma}{dy} &\equiv \rho_1(y) = \left\langle \sum_{\mathbf{i}} \delta(y - y_{\mathbf{i}}) \right\rangle, \\ \frac{1}{\sigma_{\mathbf{i}}} \frac{d^2\sigma}{dy_1 dy_2} &\equiv \rho_2(y_1, y_2) = \left\langle \sum'_{\mathbf{i}, \mathbf{j}} \delta(y_1 - y_{\mathbf{i}}) \delta(y_2 - y_{\mathbf{j}}) \right\rangle, \\ \frac{1}{\sigma_{\mathbf{i}}} \frac{d^3\sigma}{dy_1 dy_2 dy_3} &\equiv \rho_3(y_1, y_2, y_3) = \left\langle \sum'_{\mathbf{i}, \mathbf{j}, \mathbf{k}} \delta(y_1 - y_{\mathbf{i}}) \delta(y_2 - y_{\mathbf{j}}) \delta(y_3 - y_{\mathbf{k}}) \right\rangle, \end{aligned} \quad (11)$$

where ρ_q are the rapidity distribution correlation functions and the hat to the summation refers to exclusion of terms with equal indices. Eqs. (11) enable simplified calculations for the integrating the correlations from the fluctuations of the particle multiplicity considering different domains in the rapidity ranges. Assuming a domain Q_2 with equal ranges Δy of y_i , thus Eq. (8) can be rewritten as

follows [60].

$$\begin{aligned}
\int_{Q_1} \rho_1(y_1) dy_1 &= \langle N \rangle_{Q_1}, \\
\int_{Q_2} \rho_2(y_1, y_2) dy_1 dy_2 &= \langle n(n-1) \rangle_{Q_2}, \\
\int_{Q_3} \rho_3(y_1, y_2, y_3) dy_1 dy_2 dy_3 &= \langle n(n-1)(n-2) \rangle_{Q_3}.
\end{aligned} \tag{12}$$

For application in high-energy analysis, the factorial moments of the averaged bin for $\rho = 2$ can be rewritten as [59]

$$\int_{Q_2} \rho_2(y_1, y_2) dy_1 dy_2 = \sum_{k=1}^X \langle n_k(n_k-1) \rangle, \tag{13}$$

where n_k is the number of particles in bin (k). The summation over hypercubes in higher dimensions $Q_q = \sum (\delta y)^n$ gives (a generalization to Q_q):

$$\int_{Q_q} \rho_q(y_1, y_2, \dots, y_q) dy_1 dy_2 \dots dy_q = \sum_{k=1}^X \langle n_k(n_k-1) \dots (n_k-n+1) \rangle. \tag{14}$$

When removing the symmetry of low-order density correlations, the cumulants can be used. The correlation functions of the cumulants (c_p) are then to be expressed in terms of correlation densities and vice versa as the follows (number of permutations in the sums are shown in brackets) [60].

$$\begin{aligned}
\rho_2(1, 2) &= \rho_1(1) \rho_1(2) + c_2(1, 2), \\
\rho_3(1, 2, 3) &= \rho_1(1) \rho_1(2) \rho_1(3) + \sum_{(3)} c_2(1, 2) \rho_1(3) + c_3(1, 2, 3), \\
\rho_4(1, 2, 3, 4) &= \rho_1(1) \rho_1(2) \rho_1(3) \rho_1(4) + \sum_{(4)} \rho_1(1) \rho_1(2) c_2(3, 4) \\
&\quad + \sum_{(3)} c_2(1, 2) c_2(3, 4) + \sum_{(4)} c_3(1, 2, 3) \rho_1(4) + c_4(1, 2, 3, 4).
\end{aligned} \tag{15}$$

The factorial of cumulant moments (f_q) reads [59]

$$f_2 = \langle n(n-1) \rangle - \langle n \rangle^2, \tag{16}$$

$$f_3 = \langle n(n-1)(n-2) \rangle - 3 \langle n(n-1) \rangle \langle n \rangle + 2 \langle n \rangle^3, \tag{17}$$

and so on, are just integrals of the corresponding cumulants (c_p).

The moments can be then averaged over all bins, X numbers of identical widths (δy) normalized either to the overall mean number per bin, $[\bar{n} = \bar{\rho} \delta y = \sum_{m=1}^X \langle n_m \rangle / X]$ or to the local average $\langle n_m \rangle \equiv \bar{\rho}_m \delta y$. These choices are usually referred to as "horizontal" and "vertical" averages, respectively, [59]

$$F_q^h \equiv \frac{1}{X (\delta y)^q} \sum_{m=1}^X \int_{Q_m} \prod_i dy_i \frac{\rho_q(y_1 \dots y_q)}{\bar{\rho}^q}, \tag{18}$$

$$F_q^v \equiv \frac{1}{X} \sum_{m=1}^X \frac{\langle n_m (n_m - 1) \cdots (n_m - q + 1) \rangle}{\langle n_m \rangle^q}. \quad (19)$$

Recalling the factorial cumulants of the averaged bin

$$K_q^h(\delta y) \equiv \frac{1}{X} \sum_{m=1}^X \frac{f_q^m}{n^q} = \frac{1}{X (\delta y)^q} \sum_{m=1}^X \int_{Q_m} \prod_i dy_i \frac{c_q(y_1 \cdots y_q)}{\rho^q} = \sum_m \frac{N_m (N_m - 1)}{2\sqrt{\pi}\sigma_T} e^{-y^2/4\sigma_T^2}, \quad (20)$$

$$K_q^v(\delta y) \equiv \frac{1}{X} \sum_{m=1}^X \frac{f_q^m}{\langle n_m \rangle} = \frac{1}{X (\delta y)^q} \sum_{m=1}^X \int_{Q_m} \prod_i dy_i \frac{c_q(y_1 \cdots y_q)}{\langle \rho_m \rangle^q} = \sum_{m \neq m'} \frac{N_m N_{m'}}{2\sqrt{\pi}\sigma_T} e^{-(y - \bar{y}_m + \bar{y}_{m'})^2/4\sigma_T^2}. \quad (21)$$

It is obvious that when the values of one variable, such as (y_1) approaches zero, the dependence on y_2 of the correlated particle could be fitted as an either exponential or Gaussian distribution in order to deduce the cumulant K_2 [59]

$$K_2 \equiv \frac{\rho_2(y_1, y_2) - \rho_1(y_1)\rho_1(y_2)}{\rho_1(y_1)\rho_1(y_2)} \approx \gamma_2 e^{-(y_1 - y_2)^2/4\lambda^2}, \quad (22)$$

where the rapidity density of a source n emitting $\int dy \rho_1^{(m)}(y)$ particles [61]

$$\rho_1^{(n)} \approx \sum_n \frac{N_n}{\sqrt{2\pi}\sigma_T} e^{-\frac{1}{2}(y - \bar{y}_n)^2/\sigma_T^2}, \quad (23)$$

which can be directly related to dN/dy .

III. COSMIC RAY MONTE CARLO (CRMC) MODEL

As introduced, the hybrid Cosmic Ray Monte Carlo (CRMC EPOS1hc) event generator shall be utilized in generating various multiplicity per rapidity for different hadrons, at energies ranging between $\sqrt{s_{NN}} = 6.3$ and 5500 GeV. The CRMC EPOS1hc results are then compared with the available experimental data and finally fitted by the HRG and Carruthers approaches.

The CRMC is an interface for the various cosmic ray monte-carlo models for various effective quantum chromodynamic (QCD) models and different experiments such as CMS, ATLAS, LHCb, NA61 and the ultra high-energy cosmic rays observatory Pierre Auger, etc. It includes different types of interactions that are built on the highly Gribov-Regge model-like EPOS1hc/1.99. CRMC introduces a full description for background taking into consideration the resultant diffraction. Its interface can access the resultant output from various event-generators for heavy-ion collisions. CRMC interface is also connected to a wide spectrum of models, such as, qgsjet01 [44, 45], qgsjetII [46–48], sibyll [49–51] and EPOS 1.99/lhc [52, 53]. QGSJET01 and SIBYLL2.3, at low energies. EPOS lhc/1.99, QGSJETII v03 and v04 are the interaction models that can be integrated at high energies.

In the present paper, we utilize the CRMC EPOS_{lhc} event generator which contains various parameters for the primordial observables in high-energy collisions and their phenomenological assumptions. These can be modified due to theoretical and experimental postulates. It was argued that EPOS_{lhc} is able to give a reasonable description for heavy-ion collisions regarding the generated data from various experiments and also other event generators [52, 53].

EPOS_{lhc} was originally constructed for cosmic ray air showers and could be utilized for pp- and AA-collisions, at SPS, RHIC, and LHC energies. EPOS_{lhc} even uses a more simplified treatment for heavy-ion collisions at the last stage of their evolutions and thus can be applied for minimum bias in the interactions between hadrons in the nuclear collisions [62]. EPOS_{lhc} is a parton model with various parton-parton interactions resulting in various parton ladders and provides a good estimation for particle yields, multiple scattering of partons, evaluations of cross-section, shadowing and screening through splitting and unitarization, and various collective effects of hot and dense media. It should be mentioned that EPOS_{lhc} does not consider the simulations for complete hydro system even in the last stage.

In the present work, we utilize EPOS_{lhc} event generator, at energies spanning between 6.3 and 5500 GeV for an ensemble of at least 100,000 events. We have calculated the multiplicity for π^- , π^+ , k^- , k^+ , \bar{p} , p , and $p - \bar{p}$ in various rapidity windows $-6 < y < 6$. Proving the validity of the hybrid EPOS_{lhc} event generator, we hope at calculating the multiplicity per rapidity for the considered various hadrons, which is assumed to come up with a novel input for the future facilities NICA and FAIR, for instance.

IV. RESULTS AND DISCUSSION

The present analysis is based on a reproduction of experiments results for the multiplicity per rapidity dN/dy of π^- , π^+ , k^- , k^+ , \bar{p} , p , and $p - \bar{p}$ [32–34, 36–41], at energies ranging between 6.3 and 5500 GeV. We also compare with results deduced from EPOS_{lhc} event generator [52, 53]. Both sets of results are then confronted to the HRG thermal and the Carruthers rapidity approaches, in which the dependence of the freezeout temperature T and the baryon-chemical potential μ_B on the centre-of-mass energy $\sqrt{s_{NN}}$ is taken from ref. [1].

The present work aims at updating the study of the multiplicity per rapidity in the HRG model. One of the improvements we are presenting here is the inclusion of various missing states to the well-known hadron states recently reported by the particle data group [54]. The missing states are hadron

resonances which are theoretically predicted [55], but not yet confirmed, experimentally. Various physical characteristics including masses, and other quantum numbers, etc. are theoretically well known. It was conjectured that these states greatly contribute to the fluctuations and the correlations simulated in the recent lattice QCD calculations [63]. Best reproduction of fluctuations and the correlations are among the main motivations to add these hadron states to the HRG model [64]. Regardless the corresponding limitations, we intend it check whether the new hadron states contribute to the multiplicity per rapidity of π^- , π^+ , k^- , k^+ , \bar{p} , p , and $p - \bar{p}$, as the missing states likely come up with additional degrees of freedom and certainly considerable decay channels which might affect the final number of particles produced.

Also the present work introduces a new approach based on Carruthers proposal for hierarchy of cumulant correlation functions and their linked-pair approximation, which satisfactorily characterizes the galaxy correlation and successfully describes the central rapidity domain [59]. The basic idea is an approximate translation invariance and a linking of averaged factorial moments to the second-order experimental moment in the final state of the particle production. As for rapidity histograms, it was assumed that the various bins are likely irregular, i.e. they are influenced by fractal attractor, e.g. intermittence, where the full range of rapidity $(\Delta y)^p$ is divided into smaller hypercubes of size $(\delta y)^p$. An ordinary bin-averaged factorial moments can be determined, which can then be expressed in linked-pair approximation. This - in turn - can be related to the negative binomial distribution. For the high-energy collisions, a specific functional form such as Gaussian or an exponential can be proposed for the cumulants or the correlation functions, Eq. (23).

The results obtained are compared with both experiment and event generator. For almost all particles, the dependence of the multiplicity per rapidity dN/dy on the rapidity y was fitted to Gaussian normal distribution function,

$$\frac{dN}{dy} = a_0 \exp \left\{ -0.5 \left[\left(\frac{y - a_1}{a_2} \right) \left(\frac{y - a_1}{a_2} \right) \right] \right\}, \quad (24)$$

where a_0 , a_1 , and a_2 are the fit parameters, Tab. I. For net proton $p - \bar{p}$, we use the binomial

$$\frac{dN}{dy} = c_0 + c_1 y + c_2 y^2 + c_3 y^3, \quad (25)$$

in which c_0 , c_1 , c_2 , and c_3 are free parameters, Tab. II.

Figure 1 shows the multiplicity per rapidity dN/dy versus y in a semi-log scale. The experimental results for π^- , π^+ , k^- , k^+ , \bar{p} , p , and $p - \bar{p}$ [32–34, 36–41] (symbols) are compared with the CRMC EPOS1hc event generator [52, 53] (dashed curves). At the Large Hadron Collider (LHC) energies, 2760 and 5500 GeV, we introduce CRMC predictions. To the authors best knowledge, there is not such

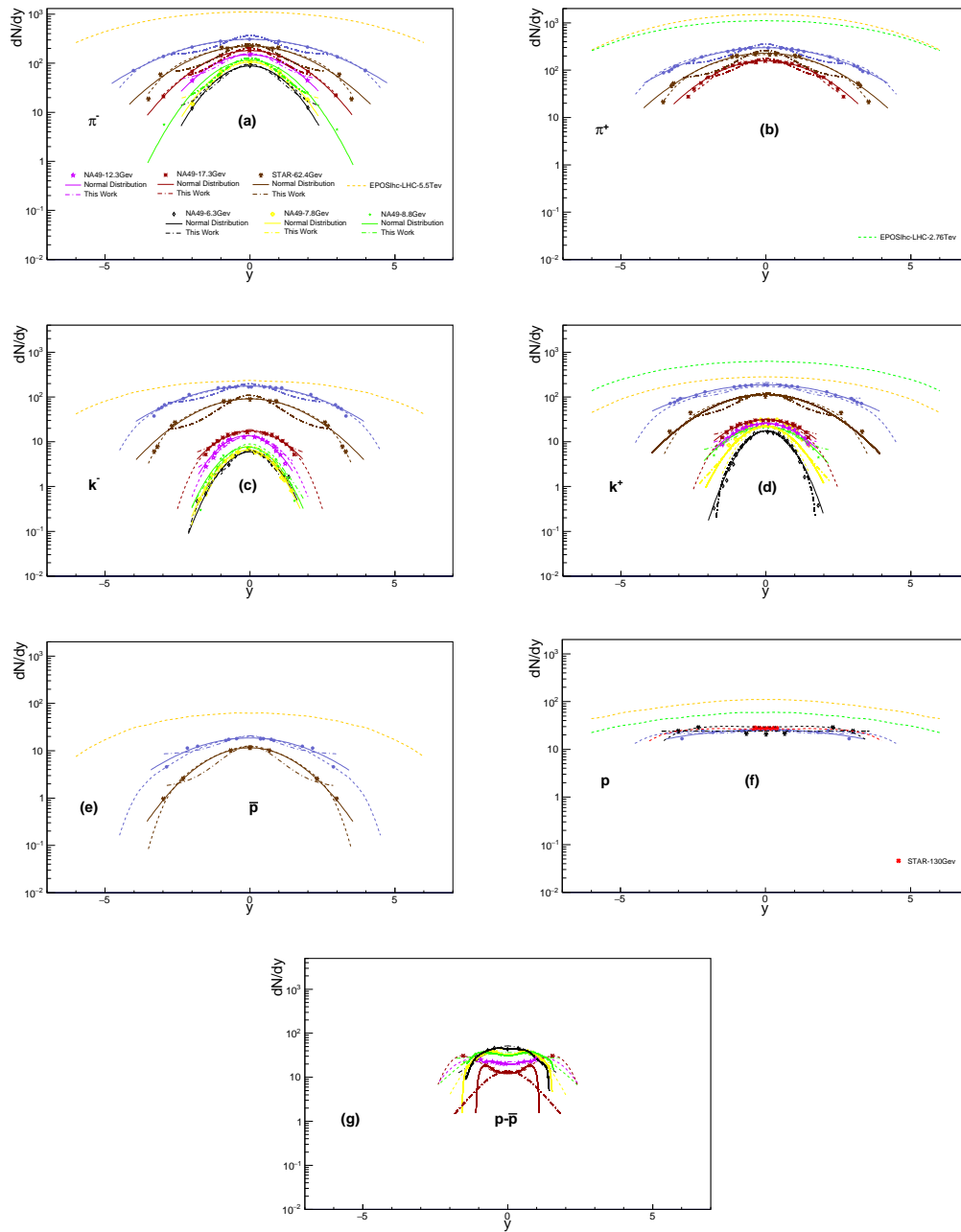


Fig. 1: (Color online) In semi-log scale, the multiplicity per rapidity for π^- , π^+ , k^- , k^+ , \bar{p} , p , and $p-\bar{p}$ particle yields is depicted as a function of the rapidity. The experimental results [32–34, 36–41] (symbols) are compared to the Cosmic Ray Monte-carlo (CRMC EPOS1hc) event generator (dashed curves), section III, and also fitted to the hadron resonance gas (HRG) approach (dash-dotted curves), Eq. (6) or Eq. (7) and to the Gaussian distribution function (solid curve).

measurements to depict and compare with. The experimental results are fitted to the hadron resonance gas (HRG) approach (dash-dotted curves), Eq. (6) or Eq. (7) and to the Gaussian distribution function

(solid curve). For a better comparison, we keep the same dN/dy - and y -scales in all panels devoted to the different particle yields.

There is a general observation that for all particles when the energy decreases, especially from top RHIC down to low SPS, i.e. from 200 down to 6.3 GeV, when disregarding our CRMC-predictions at LHC energies, the statistical fits seem becoming better and better. \bar{p} and $p - \bar{p}$ are exceptions. Their fits become worse with decreasing the energy. Also, we generally observe that the HRG model can excellently describe the experimental/simulation results up to a relative narrow range around mid-rapidity. For a wider y -range, the ability of the HRG model to reproduce the results deduced from the experiments and the simulations becomes more and more worse. These are generic observations, from which final conclusions can be drawn. The goodness of the statistical fits shall be estimated, quantitatively. We find that the results from the CRMC EPOS_{lhc} event generator match well with the experimental results. Accordingly, we present predictions, at LHC energies. Also, we observe that dN/dy for the net-proton $p - \bar{p}$ seems to have two peaks. This might be understood due to the binomial assumed for this particle yield. For π^- , π^+ , k^- , k^+ , \bar{p} , and p , the fit parameters V and m_T , i.e. the volume of the fireball and the mass of the particle, respectively, are listed in Tab. I. For net-proton $p - \bar{p}$, the corresponding fit parameters as deduced from Eq. (25) are given in Tab. II.

Figure 2 shows dN/dy versus y from Carruthers rapidity approach, Eq. (23), and CRMC EPOS_{lhc} event generator compared with the experimental data [32–34, 36–41]. We conclude that the results on dN/dy excellently agree well with the CRMC EPOS_{lhc} event generator. The agreement with CRMC is also excellent. The goodness of corresponding fits is outlined in Tab. I.

In light of this, we conclude that the correlations and fluctuations of the particle multiplicity as included in the Carruthers approach are essential for a better reproduction of the rapidity distributions of the various particles. The latter are likely isotropic and hence the overall results apparently match well with the Gaussian normal distribution. The corresponding parameters γ_2 , \bar{y}^n , and σ_m can be related to the resulting fit parameters, $\gamma_2 = a_0$, $\bar{y}^n = a_1$, and $\sigma_m = a_2$, Eq. (24).

The multiplicity per rapidity of the well-identified particles π^- , π^+ , k^- , k^+ , \bar{p} , p , and $p - \bar{p}$ measured in various high-energy experiments, at energies ranging from 6.3 to 5500 GeV, are successfully compared to the Cosmic Ray Monte Carlo (CRMC) event-generator. The Carruthers and hadron resonance gas approaches are then fitted to both sets of results. We found that the Carruthers approach reproduces well the full range of multiplicity per rapidity for all produced particles, at the various energies, while the HRG approach fairly describes the results within a narrower rapidity-range.

particle	$\sqrt{S_{NN}}GeV$	a_0	a_1	a_2	χ^2/dof	V	m_T
π^-	200	308.369 ± 0.584	$-4.752 \times 10^{-3} \pm 5.107 \times 10^{-3}$	$2.341 \pm 5.661 \times 10^{-3}$	0.888	$2.536 \times 10^5 \pm 1.006 \times 10^4$	0.134 ± 0.067
	62.4	226.487 ± 4.722	$1.711 \times 10^{-3} \pm 7.783 \times 10^{-2}$	$1.778 \pm 6.893 \times 10^{-2}$	120.8	$2.938 \times 10^5 \pm 7.193 \times 10^4$	0.052 ± 0.026
	17.3	180.989 ± 0.581	$-6.108 \times 10^{-6} \pm 5.299 \times 10^{-3}$	$1.436 \pm 5.371 \times 10^{-3}$	0.568	$3.188 \times 10^5 \pm 7.985 \times 10^4$	0.035 ± 0.017
	12.3	148.9 ± 0.598	$-1.595 \times 10^{-3} \pm 5.926 \times 10^{-3}$	$1.279pm6.479 \times 10^{-3}$	0.518	$2.598 \times 10^5 \pm 5.951 \times 10^4$	0.041 ± 0.018
	8.8	115.246 ± 0.999	$4.526 \times 10^{-4} \pm 1.136 \times 10^{-2}$	$1.135 \pm 1.152 \times 10^{-2}$	1.342	$1.937 \times 10^5 \pm 3.076 \times 10^4$	0.018 ± 0.009
	7.8	104.838 ± 1.835	$8.039 \times 10^{-3} \pm 2.104 \times 10^{-2}$	$1.045 \pm 2.086 \times 10^{-2}$	4.144	$3.195 \times 10^5 \pm 5.827 \times 10^4$	0.013 ± 0.008
	6.3	88.074 ± 0.272	$4.068 \times 10^{-3} \pm 3.567 \times 10^{-3}$	$1.004 \pm 3.554 \times 10^{-3}$	0.086	$3.492 \times 10^5 \pm 5.019 \times 10^4$	0.009 ± 0.005
π^+	200	298.692 ± 1.479	$-2.327 \times 10^{-4} \pm 1.348 \times 10^{-2}$	$2.265 \pm 1.445 \times 10^{-2}$	17.22	$2.691 \times 10^5 \pm 4.3869 \times 10^4$	0.120 ± 0.026
	62.4	-490.308 ± 0.025	-0.051 ± 0.03	1.826 ± 2.588	31.15	$3.024 \times 10^5 \pm 7.809 \times 10^4$	0.053 ± 0.025
	17.3	159.21 ± 1.932	$2.579 \times 10^{-3} \pm 2.28 \times 10^{-2}$	$1.548 \pm 2.499 \times 10^{-2}$	27.441	$2.098 \times 10^5 \pm 3.376 \times 10^4$	0.068 ± 0.017
κ^-	200	907.015 ± 12.609	$3.379 \times 10^{-3} \pm 0.033$	$2.066 \pm 3.294 \times 10^{-2}$	34.44	$1.477 \times 10^5 \pm 2.845 \times 10^4$	0.1210 ± 0.0329
	62.4	358.495 ± 8.401	$2.049 \times 10^{-3} \pm 4.630 \times 10^{-2}$	$1.570 \pm 3.731 \times 10^{-2}$	12.304	$1.587 \times 10^5 \pm 2.315 \times 10^4$	0.026 ± 0.009
	17.3	17.505 ± 0.353	$1.311 \times 10^{-3} \pm 1.95 \times 10^{-2}$	$1.0673 \pm 2.692 \times 10^{-2}$	0.472	$2.922 \times 10^5 \pm 3.251 \times 10^4$	0.035 ± 0.009
	12.3	13.679 ± 0.357	$-0.119 \pm 1.867 \times 10^{-2}$	$0.833 \pm 2.344 \times 10^{-2}$	0.374	$3.189 \times 10^5 \pm 4.360 \times 10^4$	0.009 ± 0.007
	8.8	7.643 ± 0.247	$-9.317 \times 10^{-2} \pm 2.101 \times 10^{-2}$	$0.769 \pm 2.184 \times 10^{-2}$	0.136	$2.656 \times 10^5 \pm 2.3145 \times 10^4$	0.002 ± 0.003
	7.8	6.499 ± 0.130	$-8.229 \times 10^{-2} \pm 1.530 \times 10^{-2}$	$0.738 \pm 1.586 \times 10^{-2}$	0.057	$2.484 \times 10^5 \pm 1.480 \times 10^4$	0.003 ± 0.002
	6.3	5.961 ± 0.185	$3.077 \times 10^{-3} \pm 2.162 \times 10^{-2}$	$0.732 \pm 2.369 \times 10^{-2}$	0.097	$2.811 \times 10^5 \pm 1.169 \times 10^4$	0.003 ± 0.001
k^+	200	187.765 ± 0.926	$-2.151 \times 10^{-4} \pm 1.539 \times 10^{-2}$	$2.383 \pm 1.731 \times 10^{-2}$	6.996	$1.183 \times 10^5 \pm 1.929 \times 10^4$	0.197 ± 0.0414
	62.4	222.355 ± 119.846	-0.926 ± 55.266	0.807 ± 51.701	33.128	$1.348 \times 10^5 \pm 3.187 \times 10^4$	0.061 ± 0.026
	17.3	31.241 ± 0.547	$1.127 \times 10^{-2} \pm 2.458 \times 10^{-2}$	$1.217 \pm 3.665 \times 10^{-2}$	1.736	$3.489 \times 10^5 \pm 5.374 \times 10^4$	0.083 ± 0.021
	12.3	25.626 ± 0.364	$-1.253 \times 10^{-3} \pm 1.743 \times 10^{-2}$	$1.093 \pm 2.373 \times 10^{-2}$	0.695	$4.268 \times 10^5 \pm 4.493 \times 10^4$	0.043 ± 0.009
	8.8	21.825 ± 0.4389	$-2.923 \times 10^{-2} \pm 2.497 \times 10^{-2}$	$1.1218 \pm 2.821 \times 10^{-2}$	1.003	$4.907 \times 10^5 \pm 5.905 \times 10^4$	0.029 ± 0.007
	7.8	21.775 ± 0.261	$1.206 \times 10^{-3} \pm 9.304 \times 10^{-3}$	$0.8289 \pm 1.197 \times 10^{-2}$	0.231	$8.088 \times 10^5 \pm 2.585 \times 10^4$	0.009 ± 0.001
	6.3	17.649 ± 0.407	$4.083 \times 10^{-2} \pm 1.434 \times 10^{-2}$	$0.665 \pm 1.475 \times 10^{-2}$	0.528	$8.996 \times 10^5 \pm 3.806 \times 10^4$	0.006 ± 0.001
\bar{p}	200	18.564 ± 0.432	$-2.735 \times 10^{-3} \pm 6.479 \times 10^{-2}$	$1.937 \pm 7.527 \times 10^{-2}$	1.131	$1.336 \times 10^5 \pm 3.851 \times 10^4$	0.158 ± 0.063
	62.4	11.551 ± 0.059	$-1.265 \times 10^{-4} \pm 1.416 \times 10^{-2}$	$1.326 \pm 1.149 \times 10^{-2}$	0.017	$1.901 \times 10^5 \pm 1.986 \times 10^4$	0.021 ± 0.008
p	200	25.742 ± 0.539	$-8.487 \times 10^{-4} \pm 0.165$	3.617 ± 0.3166	2.433	$3.923 \times 10^5 \pm 7.8515 \times 10^4$	1.363 ± 0.322
	130	400.26 ± 0.285	0.984 ± 0.313	0.372 ± 0.03	34.071	$7.507 \times 10^5 \pm 3.456 \times 10^4$	9.11 ± 4.149
	62.4	24.232 ± 1.565	$-4.802 \times 10^{-2} \pm 14.652$	21.231 ± 16.460	16.75	$4.001 \times 10^5 \pm 3.587 \times 10^4$	15.015 ± 13.465

Tab. I: The fit parameters obtained from the HRG approach for rapidity distributions for π^- , π^+ , k^- , k^+ , \bar{p} and p , at various energies.

V. CONCLUSIONS

We have calculated the multiplicity per rapidity dN/dy for the well-identified hadrons π^- , π^+ , k^- , k^+ , \bar{p} , p , and $p - \bar{p}$ using two different approaches, namely HRG; a well-known framework based on thermal statistical assumptions and Carruthers approach based on correlations and fluctuations for hierarchy of the cumulant correlation functions and their linked-pair approximation, which in turn could be connected to negative binomial distributions and accordingly Gaussian- or exponential-like expressions for the rapidity distributions have been introduced.

The Carruthers and HRG approaches are then fitted to measurements at energies ranging from

particle	$\sqrt{S_{NN}}\text{GeV}$	c_0	c_1	c_2	c_3	χ^2/dof	V	m_T
$p - \bar{p}$	17.3	12.853 ± 0.762	17.501 ± 0.0726	-17.938 ± 0.064	-140.123 ± 0.583	4.454	$2.955 \times 10^5 \pm 6.042 \times 10^4$	15.579 ± 31.851
	12.3	20.002 ± 2.420	-1.913 ± 0.035	2.623 ± 0.053	18.509 ± 1.834	6.260	$3.928 \times 10^5 \pm 1.546 \times 10^4$	14.673 ± 57.729
	8.8	31.264 ± 0.579	-1.786 ± 0.564	19.819 ± 1.876	17.579 ± 1.757	4.687	$1.229 \times 10^5 \pm 7.0573 \times 10^4$	0.566 ± 0.392
	7.8	32.135 ± 1.551	-2.197 ± 0.254	37.869 ± 2.675	10.992 ± 1.565	3.156	$9.241 \times 10^5 \pm 2.020 \times 10^4$	0.039 ± 0.016
	6.3	44.269 ± 2.185	-7.632 ± 0.754	6.814 ± 0.476	39.223 ± 2.869	7.367	$1.874 \times 10^5 \pm 2.684 \times 10^4$	0.009 ± 0.006

Tab. II: The same as in Tab. I but for net-proton $p - \bar{p}$.

6.3 to 5500 GeV and to corresponding simulations from the Cosmic Ray Monte Carlo (CRMC) event generator. The excellent agreement between the measurements and the simulations provides us with framework to compare between both approaches. We found that in the full range of rapidity, the multiplicity per rapidity is successfully reproduced in the Carruthers approach. The possible fluctuations and correlations as included in it seem to assure that the produced particles become isotropically distributed. On the other hand, the HRG approach restrictedly reproduces these anisotropic distributions. Accordingly, we conclude that the statistical assumptions alone - as included in the HRG approach - wouldn't be able to apply on a wide range of rapidity. Ingredients assuring fluctuations and correlations, such as flow and interactions, if integrated in the HRG approach would likely assure a better reproduction of the multiplicity per rapidity.

Acknowledgements

The work of AT was supported by the ExtreMe Matter Institute (EMMI) at the GSI Helmholtz Centre for Heavy Ion Research.

-
- [1] A. N. Tawfik, Int. J. Mod. Phys. **A29**, 1430021 (2014).
 - [2] H. Satz, Rept. Prog. Phys. **63**, 1511 (2000).
 - [3] B. Muller, Rept. Prog. Phys. **58**, 611 (1995).
 - [4] E. V. Shuryak, Phys. Rept. **61**, 71 (1980).
 - [5] J. Cleymans, K. Redlich, H. Satz, and E. Suhonen, Z. Phys. **C33**, 151 (1986).
 - [6] J. Cleymans and H. Satz, Z. Phys. **C57**, 135 (1993).
 - [7] H. Kouno and F. Takagi, Z. Phys. **C42**, 209 (1989).
 - [8] A. Andronic, P. Braun-Munzinger, J. Stachel, and M. Winn, Phys. Lett. **B718**, 80 (2012).
 - [9] S. K. Tiwari, P. K. Srivastava, and C. P. Singh, J. Phys. **G40**, 045102 (2013).
 - [10] P. K. Srivastava and C. P. Singh, Phys. Rev. **D85**, 114016 (2012).

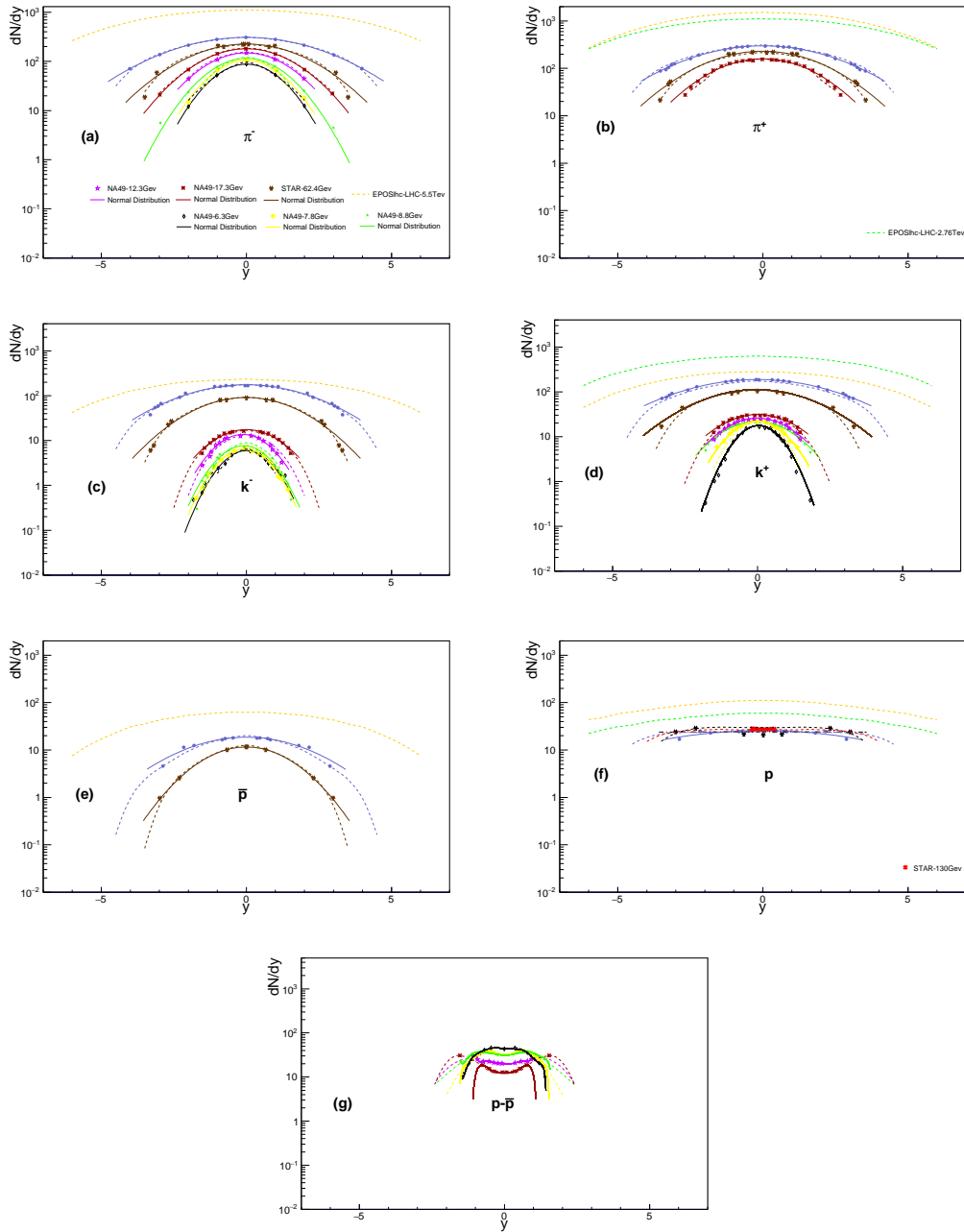


Fig. 2: The same as in fig.(1) but here for Carruthers rapidity approach.

- [11] R. Hagedorn and J. Rafelski, Phys. Lett. **97B**, 136 (1980).
- [12] L. Marques, J. Cleymans, and A. Deppman, Phys. Rev. **D91**, 054025 (2015).
- [13] S. K. Tiwari, P. K. Srivastava, and C. P. Singh, Phys. Rev. **C85**, 014908 (2012).
- [14] J. D. Bjorken, Phys. Rev. **D27**, 140 (1983).
- [15] E. Schnedermann and U. W. Heinz, Phys. Rev. Lett. **69**, 2908 (1992).
- [16] E. Schnedermann, J. Sollfrank, and U. W. Heinz, Phys. Rev. **C48**, 2462 (1993).

- [17] P. Braun-Munzinger, J. Stachel, J. P. Wessels, and N. Xu, Phys. Lett. **B365**, 1 (1996).
- [18] P. Braun-Munzinger, J. Stachel, J. P. Wessels, and N. Xu, Phys. Lett. **B344**, 43 (1995).
- [19] S.-Q. Feng and Y. Zhong, Phys. Rev. **C83**, 034908 (2011).
- [20] S. Feng and X. Yuan, Sci. China **G52**, 198 (2009).
- [21] S. Uddin, J. S. Ahmad, W. Bashir, and R. A. Bhat, J. Phys. **G39**, 015012 (2012).
- [22] T. Hirano, K. Morita, S. Muroya, and C. Nonaka, Phys. Rev. **C65**, 061902 (2002).
- [23] K. Morita, S. Muroya, C. Nonaka, and T. Hirano, Phys. Rev. **C66**, 054904 (2002).
- [24] J. Manninen, E. L. Bratkovskaya, W. Cassing, and O. Linnyk, Eur. Phys. J. **C71**, 1615 (2011).
- [25] U. Mayer and U. W. Heinz, Phys. Rev. **C56**, 439 (1997).
- [26] W. Broniowski and W. Florkowski, Phys. Rev. Lett. **87**, 272302 (2001).
- [27] W. Broniowski and W. Florkowski, Phys. Rev. **C65**, 064905 (2002).
- [28] P. Bozek, Phys. Rev. **C77**, 034911 (2008).
- [29] F. Becattini and J. Cleymans, J. Phys. **G34**, S959 (2007).
- [30] J. Cleymans, J. Strumpfer, and L. Turko, Phys. Rev. **C78**, 017901 (2008).
- [31] A. N. Tawfik, M. A. Wahab, H. Yassin, and H. N. E. Din, (2019).
- [32] J. H. Lee et al., J. Phys. **G30**, S85 (2004).
- [33] S. V. Afanasiev et al., Phys. Rev. **C66**, 054902 (2002).
- [34] I. G. Bearden et al., Phys. Rev. **C66**, 044907 (2002).
- [35] B. Biedron and W. Broniowski, Phys. Rev. **C75**, 054905 (2007).
- [36] E. L. Bratkovskaya et al., J. Phys. Conf. Ser. **878**, 012018 (2017).
- [37] J. Adams et al., Phys. Rev. **C70**, 041901 (2004).
- [38] W.-P. Zhou, S.-H. Cai, and Z.-W. Long, Chin. Phys. **C33**, 10 (2009).
- [39] K. Hebeler, S. K. Bogner, R. J. Furnstahl, A. Nogga, and A. Schwenk, Phys. Rev. **C83**, 031301 (2011).
- [40] I. G. Bearden et al., Phys. Rev. Lett. **94**, 162301 (2005).
- [41] P. Seyboth et al., Acta Phys. Polon. **B36**, 565 (2005).
- [42] C. Adler et al., Phys. Rev. Lett. **87**, 262302 (2001).
- [43] K. Adcox et al., Phys. Rev. **C69**, 024904 (2004).
- [44] N. N. Kalmykov, S. S. Ostapchenko, and A. I. Pavlov, Nucl. Phys. Proc. Suppl. **52**, 17 (1997).
- [45] N. N. Kalmykov and S. S. Ostapchenko, Phys. Atom. Nucl. **56**, 346 (1993), [Yad. Fiz.56,no.3,105(1993)].
- [46] S. Ostapchenko, Phys. Rev. **D74**, 014026 (2006).
- [47] S. Ostapchenko, Nucl. Phys. Proc. Suppl. **151**, 143 (2006).
- [48] S. Ostapchenko, AIP Conf. Proc. **928**, 118 (2007).
- [49] J. Engel, T. K. Gaisser, T. Stanev, and P. Lipari, Phys. Rev. **D46**, 5013 (1992).
- [50] R. S. Fletcher, T. K. Gaisser, P. Lipari, and T. Stanev, Phys. Rev. **D50**, 5710 (1994).
- [51] E.-J. Ahn, R. Engel, T. K. Gaisser, P. Lipari, and T. Stanev, Phys. Rev. **D80**, 094003 (2009).
- [52] K. Werner, F.-M. Liu, and T. Pierog, Phys. Rev. **C74**, 044902 (2006).

- [53] T. Pierog and K. Werner, Nucl. Phys. Proc. Suppl. **196**, 102 (2009).
- [54] M. Tanabashi et al., Phys. Rev. **D98**, 030001 (2018).
- [55] S. Capstick and N. Isgur, Phys. Rev. **D34**, 2809 (1986), [AIP Conf. Proc.132,267(1985)].
- [56] A. N. Tawfik, H. Yassin, and E. R. A. Elyazeed, (2019).
- [57] A. N. Tawfik, Adv. High Energy Phys. **2019**, 4604608 (2019).
- [58] A. N. Tawfik and E. Abbas, Phys. Part. Nucl. Lett. **12**, 521 (2015).
- [59] P. Carruthers, Proceedings of the XIII Warsaw symposium on Elementary Particle Physics , 317 (1990).
- [60] P. Carruthers, H. C. Eggers, Q. Gao, and I. Sarcevic, Int. J. Mod. Phys. **A6**, 3031 (1991).
- [61] J. Randrup, Acta Phys. Hung. **A22**, 69 (2005).
- [62] T. Pierog, I. Karpenko, J. M. Katzy, E. Yatsenko, and K. Werner, Phys. Rev. **C92**, 034906 (2015).
- [63] A. Bazavov et al., Phys. Rev. Lett. **113**, 072001 (2014).
- [64] P. Man Lo, M. Marczenko, K. Redlich, and C. Sasaki, Eur. Phys. J. **A52**, 235 (2016).